Online ISSN: 2981-0396 Print ISSN: 2981-0388

International Journal of Iron & Steel Society of Iran

Journal Homepage: https://journal.issiran.com/

Research Article

Isothermal Kinetic Analysis of Dissolution of The Retained Delta Ferrite in AISI 304 Stainless Steel During Homogenization

F. Aghebatkheiri [1], A. R. Mashreghi *[2], S. Hasani [3]

Department of Mining and Metallurgical Engineering, Yazd University, Yazd, Iran

ARTICLE INFO

Keywords:

Retained Delta Ferrite, Aisi-304 Austenitic Stainless Steel, Homogenization, Isothermal Kinetic Analysis, Fitting Models.

Article history:

Received 23 April 2024
Received in revised form 15 July 2024
Accepted 12 November 2024

ABSTRACT

In this investigation, the dissolution kinetics of delta ferrite in AISI-304 austenitic stainless steel during homogenization was studied. The study encompasses a temperature range of 1050 to 1250 °C (1523 K) and a time span from 1 to 12 hours, with hourly intervals. Utilizing MIP software, the delta ferrite content in the homogenized steel was quantified. The findings demonstrate a reduction in delta ferrite content as both annealing temperature and duration increase. The presence of delta ferrite in AISI-304 steel is undesirable, and homogenization proves effective in minimizing this phase, thereby enhancing mechanical properties. The dissolution of delta ferrite and chromium carbide, along with grain growth, contributes to a decrease in hardness throughout the homogenization process. Furthermore, kinetic analysis in isothermal conditions was performed to determine the parameters governing this phenomenon using the Arrhenius model. The activation energy (E) and pre-exponential factor (A) were determined to be 246.14 kJ/mol and 8.28×10^{7} hr^{-1}, respectively. Also, the results suggested that this process follows a two-dimensional reaction model (R2).

1. Introduction

Stainless steel, an iron-based alloy rich in chromium, often incorporates additional elements like nickel and molybdenum, resulting in various grades based on alloy composition. Among these, austenitic stainless steels stand out as the most prevalent and crucial variants. Renowned for their resistance to corrosion in diverse environments such as freshwater, seawater, acidic and alkaline solutions, and industrial settings, these steels also exhibit remarkable resilience to oxidation and chemical corrosion at elevated temperatures common in high-temperature processes [1–4].

While austenitic stainless steels typically exhibit a single austenite phase at room temperature, the presence of delta ferrite can arise due to solidification and manufacturing processes such as heat treatment and welding [5]. Unfortunately, the presence of delta ferrite can compromise fatigue resistance, impact toughness, tensile properties, and resistance to pitting corrosion, potentially leading to the transformation of delta ferrite into the sigma phase [6–8]. Studies have indicated that during aging, delta ferrite in austenitic stainless steel decomposes into a chromium-rich phase and secondary austenite [9–11], underscoring the need to explore the impact of delta ferrite transformation on grain boundary corrosion behavior for a comprehensive understanding of corrosion resistance.

* *Corresponding Author*
Email: amashreghi@yazd.ac.ir
Address: Department of Mining and Metallurgical Engineering, Yazd University, Yazd, Iran
1. M.S., 2. Associate Professor, 3. Associate Professor

DOI: http://10.22034/IJISSI.2024.2027052.1287
Published by ISSI (Iron & Steel Society of Iran)

Moreover, within the temperature range of 500–900°C (773 to 1173 K), carbide precipitation at the δ/γ interface can render delta ferrite a brittle intermetallic phase, detrimentally affecting the mechanical properties of the steel [7]. Delta ferrite's influence on hot ductility necessitates careful control to mitigate crack formation during hot working processes [12]. Preferably, delta ferrite removal should occur after the main casting to enhance the steel's mechanical properties [13, 14]. Industrial practices involve heating the billet at high temperatures for several hours before hot rolling to facilitate delta ferrite dissolution. However, traditional methods of delta ferrite dissolution may lead to issues such as oxidation and abnormal grain growth [15].

Given the significance of delta ferrite phase dissolution, previous studies have investigated this phenomenon. Notably, Rezayat et al. [15] conducted dissolution operations at 1150 °C (1423 K) for 6 hours, observing a decrease in delta ferrite content from 28.2% to 18.1% and highlighting the temperature's role in enhancing ferrite dissolution. Similarly, Kim and colleagues [16] studied delta ferrite dissolution in continuous casting samples across a temperature range of 1050–1200 °C (1323 to 1473 K), noting rapid initial dissolution attributed to excessive chromium reduction in delta ferrite due to carbide precipitation.

However, despite existing research, a comprehensive analysis of delta ferrite dissolution behavior during heat treatment in AISI-304 stainless steel using the homogenization process remains scarce. This study aims to address this gap by employing a single-load or ingot casting method to produce samples, potentially yielding more stable ferrite during solidification. Unlike continuous casting methods, which may produce finer ferrite with lower volume percentages, the selected method allows for controlled delta ferrite formation, catering to specific applications. By subjecting austenitic stainless steel to the homogenization process, efforts are made to significantly reduce the delta ferrite phase. Additionally, this study delves into the kinetics of the delta ferrite dissolution process, determining crucial kinetic parameters, including activation energy (E), pre-exponential factor (A), and kinetic model (g(α)) using fitting models.

2. Materials and Methods

2.1. Materials and Sample Preparation

The material investigated in this study was sourced from a 40×40×200 cm³ ingot cast by Iran Alloy Steel Company. The chemical analysis of the steel, conducted using a quantometer device, is presented in Table 1.

AISI-304L austenitic stainless steel, characterized by its fully austenitic structure, exhibits delta ferrite phase formation during casting and welding due to segregation during solidification, influenced by the Cr/Ni ratio. The chemical homogenization process can mitigate the presence of this phase. To explore the impact of temperature and homogenization duration on delta ferrite dissolution kinetics, homogenization was performed isothermally within the temperature range of 1050–1250 °C (1323 to 1473 K) for durations ranging from 1 to 12 hours under an air atmosphere. Subsequently, the samples underwent quenching in cold water. Samples measuring 1 cm³ were utilized to assess the various stages of the dissolution process.

2.2. Characterization

The microstructure of the steel was examined using standard metallographic techniques. Samples were categorized into four groups and prepared by sanding the surface with SiC sandpaper of varying grades from 60 to 2500. Polishing was carried out using 3 μm alumina powder, followed by etching with a marble etching solution (10 ml HCl + 13 ml H_2O + 1 g $CuSO_4$). Microstructural analysis was performed using an optical microscope (OM, Olympus BX60M), and the percentage of the ferrite phase was determined using MIP software. Hardness measurements were conducted using the Brinell method with an INSTRON hardness tester applying a force of 187.5 kg, and hardness variations were plotted against temperature and time. The hardness reported for each sample is the average of five hardness tests.

2.3. Kinetic Analysis

The study of solid-state reaction kinetics dates back to

Table 1. Chemical Composition of AISI-304L Stainless Steel.

V	Ni	Mo	Cr	Mn	Si	C
0.051	8.815	0.191	18.388	0.909	0.46	0.019
W	**N**	**Al**	**Ti**	**Co**	**Cu**	**Fe**
0.018	0.032	0.006	0.002	0.083	0.322	Balanced

the early 20th century, with experimental techniques like differential thermal analysis (DTA) [17–19], differential scanning calorimetry (DSC) [20–22], thermogravimetric analysis (TG) [23, 24], and dilatometry (DIL) [25], etc. Initial kinetic studies were conducted under isothermal conditions, with non-isothermal methods gaining prominence later [26]. Flynn's [27] work on non-isothermal kinetics introduced the concept of temperature-dependent rate constants and reaction mechanisms. The Arrhenius equation, a fundamental model in kinetics, relates the rate constant to temperature and activation energy. Kinetic studies in isothermal conditions have been extensively explored using fitting models, as demonstrated by Vitazek et al. [28] in their investigation of wood thermal decomposition kinetics. The degree of reaction progress (α) is calculated based on the initial and final volume fractions of delta ferrite in the sample, aiding in determining reaction kinetics. The integral form of the reaction model (g(α)) provides insights into the reaction mechanism, with the slope of g(α) against time yielding the rate constant. Various reaction models and expressions for g(α) are available in the literature to elucidate solid-state reaction mechanisms [25–27].

3. Results and Discussion

3.1. Microstructural Observations

Fig. 1. illustrates the effect of homogenizing temperature on the microstructure of the original sample. As seen, the high-temperature homogenization process facilitated the diffusion of chromium and nickel, resulting in a more uniform distribution of these elements. Consequently, the alloy structure transitioned towards the thermodynamic equilibrium of the homogenization temperature. The observations reveal a reduction in the ferrite phase and an increase in the austenite phase. Additionally, the homogenization process transformed the worm-shaped ferrite, characterized by higher surface energy, into a coaxial morphology with lower surface energy. The images indicate that, with increasing homogenization temperature at a fixed time duration, this morphological transformation occurs. As the homogenization process continues, the delta ferrite phase diminishes further, adopting a spherical shape.

The evolution of the delta ferrite volume fraction with homogenization time at different temperatures is depicted in Fig. 2. Initially, a sharp decline in the delta ferrite percentage is observed with increasing temperature, followed by a more gradual decrease.

Table 2. presents the delta ferrite phase percentages during the homogenization process. Generally, an increase in homogenization time corresponds to a decrease in the delta ferrite phase. At 1050 and 1100 °C (1323 and 1373 K), the initial reduction in the ferrite phase was minimal during the first two hours, with a more pronounced decrease thereafter. Conversely, at 1150 and 1200 °C (1423 and 1473 K), a significant reduction in the ferrite phase was observed from the outset. Notably, at 1250 °C (1523 K), a substantial reduction in the ferrite phase percentage occurred, suggesting that homogenization at this temperature for 3–4 hours effectively remove the delta ferrite phase.

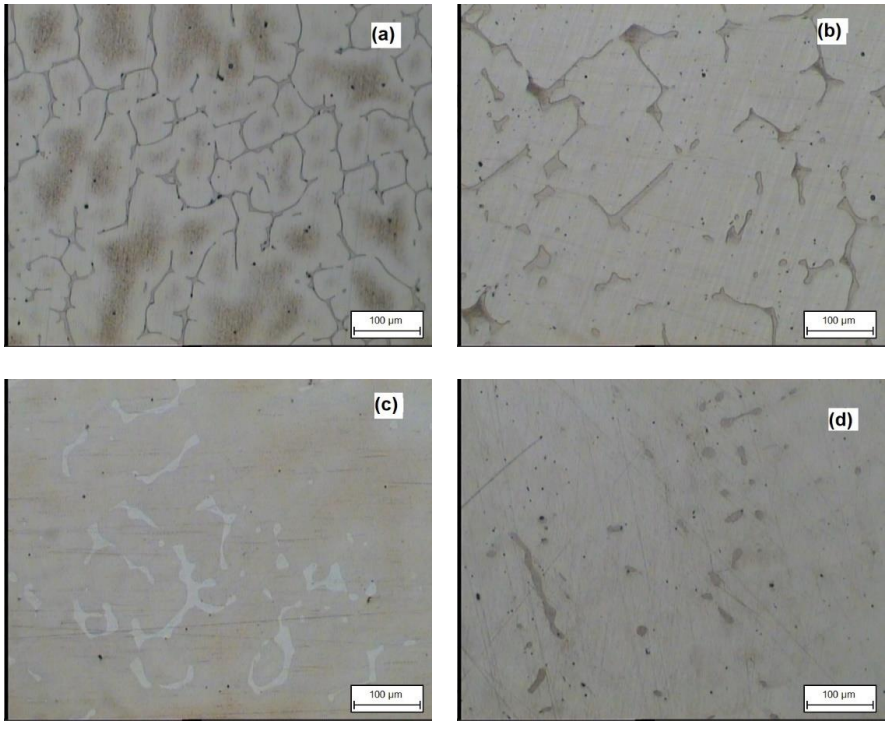

Fig. 1. The optical micrographs related to the (a) as-cast sample and specimens homogenized at (b) 1100, (c) 1150, and (d) 1200 °C for 4 hours. The volume fraction of delta ferrite is 10.2%, 7.56%, 5.25%, and 3.08%, respectively.

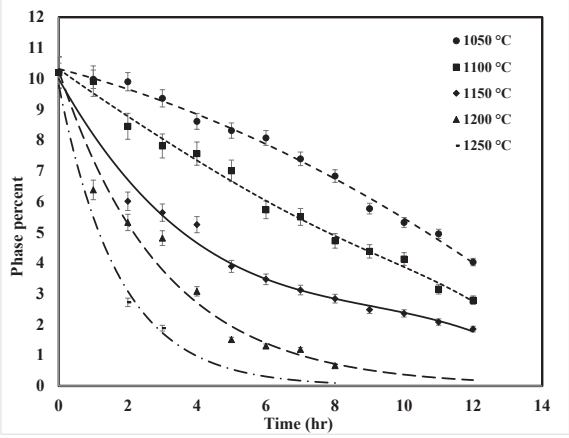

Fig. 2. Changes in the percentage of the delta ferrite phase in the investigated AISI-304 steel concerning homogenization time.

Table 2. Percentage of delta ferrite in the used AISI-304 steel after the dissolution process at various temperatures and times.

Temperature (°C) / Time (hr)	1050	1100	1150	1200	1250
0	10.2	10.2	10.2	10.2	10.2
1	9.98	9.92	7.22	6.38	2.75
2	9.9	8.45	6.01	5.32	2.72
3	9.36	7.81	5.64	4.81	1.88
4	8.61	7.56	5.25	3.08	-
5	8.31	7.25	3.89	1.51	-
6	8.07	5.73	3.47	1.3	-
7	7.39	5.5	3.12	1.19	-
8	6.83	4.72	2.84	0.66	-
9	5.77	4.38	2.48	-	-
10	5.32	4.13	2.36	-	-
11	4.95	3.15	2.08	-	-
12	4.03	2.79	1.85	-	-

Furthermore, the results of homogenization at 1100 °C (1373 K) indicated a rapid decrease in the delta ferrite phase after 2 hours, demonstrating a faster dissolution rate compared to 1050 °C (1323 K). The morphology of a considerable proportion of delta ferrite transformed from worm-shaped to coaxial. Fig. 3. illustrates the morphological changes and ferrite phase percentages at different time intervals at 1100 °C (1373 K).

3.2. Hardness

The cross-sectional hardness of the homogenized samples was evaluated at various temperatures for a constant time (refer to Fig. 4.) and at different time intervals for a constant temperature (see Fig. 5). It is evident that the hardness of the homogenized samples at a fixed time decreases with increasing temperature. This decline can be attributed to the transformation of the ferrite phase into austenite, leading to an increase in the austenite phase, as well as the dissolution of chromium carbides. The dissolution temperature of chromium carbide being below 1050 °C (1323 K) results in its gradual dissolution at temperatures higher than this threshold, with complete dissolution occurring at temperatures of 1150 °C (1423 K) and above. Consequently, this dissolution process contributes to the observed decrease in hardness. Furthermore, temperatures exceeding 1200 °C (1473 K) exhibit a more pronounced reduction in hardness, likely due to grain growth, a decrease in grain boundary density, and the dissolution of carbides of other elements present in the alloy. Given the presence of carbide-forming elements such as tungsten, vanadium, and titanium in the chemical composition of the alloy, with stronger carbide-forming tendencies than chromium, their dissolution at higher temperatures influences the hardness curve. These elements have dissolution temperatures higher than that of chromium carbide, impacting the overall hardness behavior. At a constant temperature, the hardness of the samples decreased as anticipated with increasing annealing time.

As seen in Fig. 5-a. more pronounced drop in hardness is observed during the initial 2 hours of the homogenization process. Subsequently, between 2–4 hours, the rate of hardness reduction decreases slightly, leading to a stable trend thereafter. These variations in hardness align with the changes in the percentage of the delta ferrite phase, as depicted in Fig. 2.

The analysis of hardness variations concerning temperature and time provides valuable insights into the structural evolution during homogenization and its impact on the mechanical properties of the alloy.

3.3. Dissolution Kinetics

The investigation of the dissolution kinetics of the delta ferrite phase in AISI-304 steel involved determining three key kinetic parameters. These parameters were calculated using various kinetic methods, including isothermal and non-isothermal approaches. The equation $g(\alpha)=kt$ was utilized to calculate the progress of the reaction during isothermal dissolution, with volume fraction changes considered instead of mass changes.

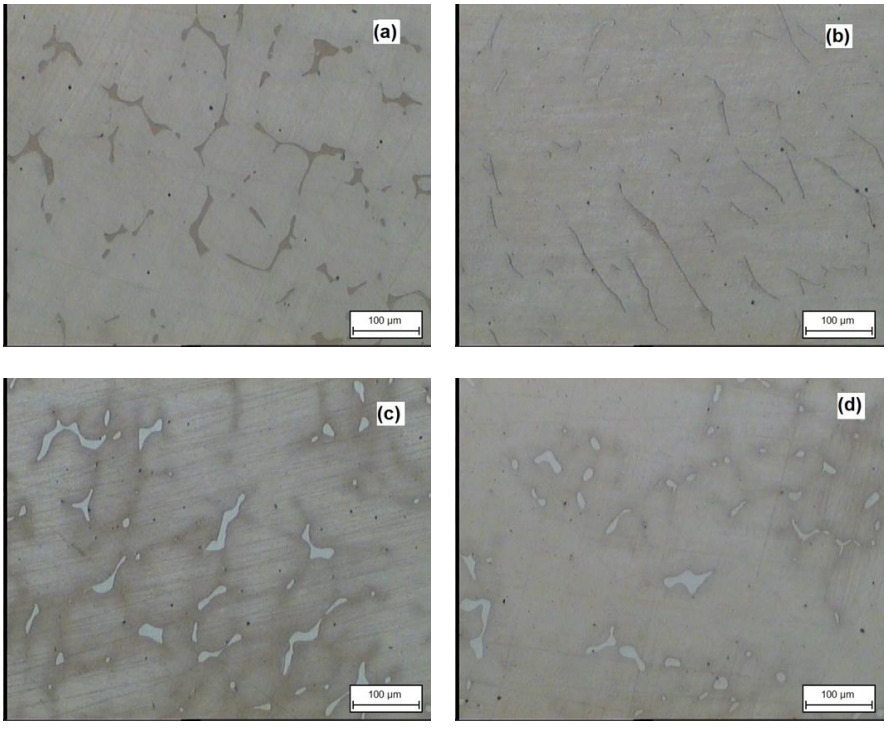

Fig. 3. The optical micrographs related to the samples annealed at 1100 °C for (a) 3, (b) 6, (c) 9, and (d) 12 hours. The volume fraction of delta ferrite is 7.81%, 5.73%, 4.38%, and 2.79%, respectively.

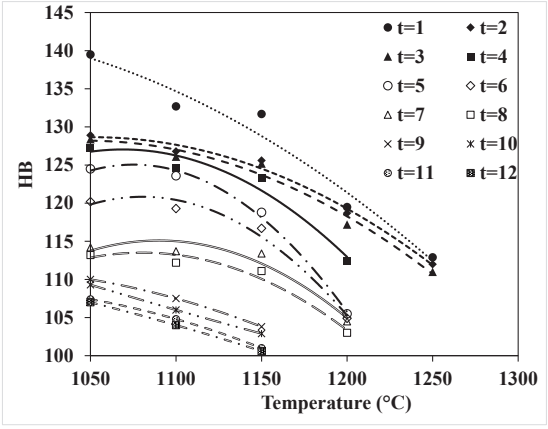

Fig. 4. Effect of homogenizing temperature on hardness.

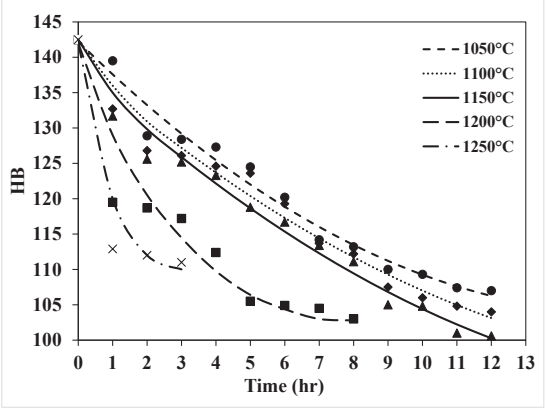

Fig. 5. Effect of homogenizing time on hardness.

By linearizing the graph of g(α) against time, the reaction mechanism and associated kinetic parameters can be deduced. The graph illustrating the fraction of the delta ferrite dissolution reaction over time at different annealing temperatures (1050 °C [1323 K], 1100 °C [1373 K], 1150 °C [1423 K], 1200 °C [1473 K], and 1250 °C [1523 K]) is presented in Fig. 6. This data was instrumental in determining the kinetic parameters.

Fig. 7. displays the linear relationship between g(α) and time for the two-dimensional reaction mechanism (R2), confirming the validity of this reaction pathway. It is noteworthy that the mechanism may vary with changes in temperature. As observed in Fig. 7. at temperatures of 1150 °C (1423 K), 1200 °C (1473 K), and 1250 °C (1523 K), the two-dimensional mechanism (R2) governs the dissolution process, indicating surface-controlled dissolution. However, at lower temperatures (1050 °C and 1100 °C [1323 K and 1373 K]), the mechanism shifts to a mixed mode, signifying a change in the reaction pathway during the course of the reaction.

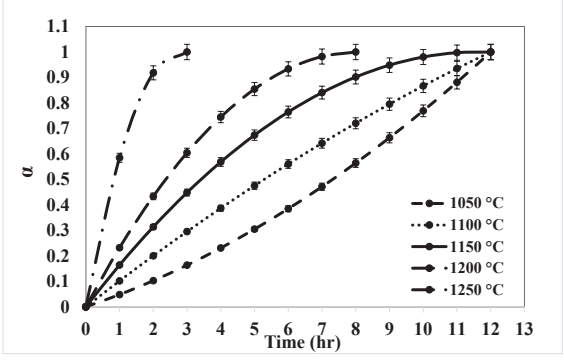

Fig. 6. Changes in the fraction of delta ferrite dissolution reaction in AISI-304 steel according to time at different temperatures.

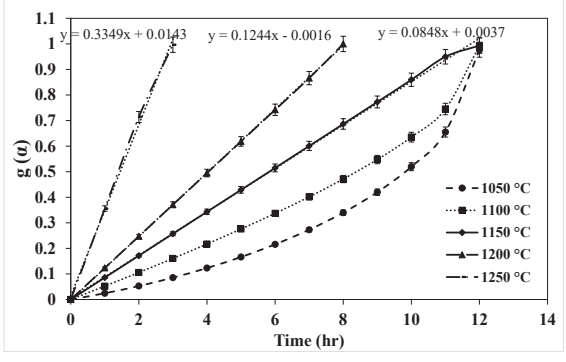

Fig. 7. Linear dependence of g(α) on reaction time for the two-dimensional reaction mechanism (R2) at different temperatures.

As mentioned, the slope of the linear graphs in Fig. 7. enables the extraction of the dissolution rate constant, as presented in Table 3.

Table 3. Calculated dissolution rate constant values at different reaction temperatures.

Homogenizing Temperature (°C)	ln k
1150	-2.46
1200	-2.08
1250	-1.09

The equation k=A.exp(-Q/RT) was utilized to determine the activation energy and the pre-exponential coefficient. The lnk curve, representing the dissolution constant k in terms of 1/T, is depicted in Fig. 8. From this curve, the activation energy and pre-exponential coefficient are calculated as 246.14 kJ.mol^{-1} and 8.28 × 10^{7} hr^{-1}, respectively.

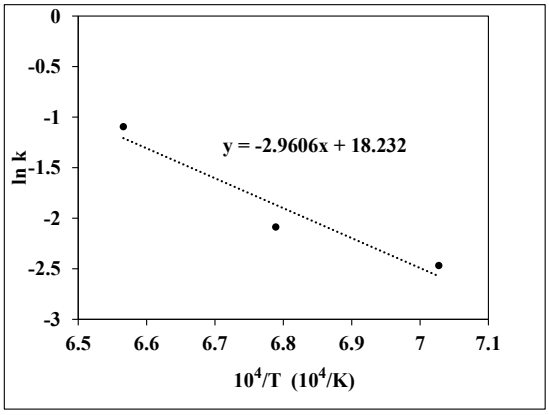

Fig. 8. Graph illustrating the logarithm of the delta ferrite dissolution rate constant in AISI-304 steel as a function of temperature.

4. Conclusions

In this study, homogenization heat treatment was conducted on AISI-304 austenitic stainless steel at temperatures ranging from 1050 to 1250 °C (1323 to 1523 K), with time intervals of 1 to 12 hours. The findings of this research shed light on several key observations:

- The investigation revealed that an increase in homogenization temperature at a constant time led to a reduction in the delta ferrite phase. Similarly, an increase in homogenization time at a fixed temperature resulted in a decrease in the delta ferrite phase due to the dissolution effect. Notably, the dissolution process exhibited a faster initial decrease in the delta ferrite phase.
- The homogenization treatment induced a transformation in the morphology of the delta ferrite phase, transitioning from a worm-like structure with higher surface energy to a coaxial appearance characterized by lower surface energy.
- Hardness measurements demonstrated that the hardness values of the samples decreased with increasing temperature at a constant time during the homogenization process. Additionally, maintaining a constant temperature while increasing the annealing time led to a reduction in sample hardness.
- Kinetic analysis was performed using the fitting models, enabling the calculation of kinetic parameters. The activation energy and pre-exponential coefficient were determined to be 246.14 kJ.mol^{-1} and 8.28×10^{7} hr^{-1}, respectively. Furthermore, the investigation revealed that the dissolution kinetics of the delta ferrite phase are governed by the R2 model.

These findings underscore the intricate interplay between homogenization parameters, microstructural evolution, mechanical properties, and kinetic behavior in the context of delta ferrite dissolution in AISI-304 steel. The comprehensive understanding gained from this study contributes to the optimization of homogenization processes and the enhancement of material properties in stainless steel applications.

References

[1] Gardner L. The use of stainless steel in structures. 2005;45–55.
[2] Plaut R.L, Herrera C, Escriba D.M, Rios P.R, Padilha A.F, A Short review on wrought austenitic stainless steels at high temperatures: processing, microstructure, properties and performance, Mater Res. 2007; 10(4): 453–60.
[3] Shen L, Wang W, Zhao W, Hui Z, Sui J, Sun P, The structure evolution of austenite stainless steel with pre-shot peening during plasma nitriding, J Phys Conf Ser. 2024; 2775(1): 012030.
[4] Jain A, Varshney A, A critical review on deformation-induced transformation kinetics of austenitic stainless steels, Mater Sci Technol. 2024; 40(2): 75–106.
[5] Bai G, Lu S, Li D, Li Y, Intergranular corrosion behavior associated with delta-ferrite transformation of Ti-modified Super304H austenitic stainless steel, Corros Sci. 2015; 90: 347–58.
[6] Rho B, The effect of δ-ferrite on fatigue cracks in 304L steels. Int J Fatigue. 2000; 22(8): 683–90.
[7] Tseng C.C, Shen Y, Thompson S.W, Mataya M.C, Krauss G, Fracture and the formation of sigma phase, M23C6, and austenite from delta-ferrite in an AlSl 304L stainless steel, Metall Mater Trans A. 1994; 25(6): 1147–58.
[8] Manning P.E, Duquette D.J, Savage W.F, The Effect of Retained Ferrite on Localized Corrosion in Duplex 304 L Stainless Steel, Weld J. 1980; 59(9): 260.
[9] Devine T.M, Mechanism of Intergranular Corrosion and Pitting Corrosion of Austenitic and Duplex 308 Stainless Steel, J Electrochem Soc. 1979; 126(3): 374–85.
[10] Soleymani S, Ojo O.A, Richards N, Effect of Composition on the Formation of Delta Ferrite in 304L Austenitic Stainless Steels During Hot Deformation, J Mater Eng Perform. 2015; 24(1): 499–504.
[11] Hsieh C.C, Wu W, Overview of Intermetallic Sigma Phase Precipitation in Stainless Steels, ISRN Metall. 2012; 2012: 1–16.
[12] Fukumoto S, Iwasaki Y, Motomura H, Fukuda Y, Dissolution behavior of δ -ferrite in continuously cast slabs of SUS304 during heat treatment, ISIJ Int. 2012; 52(1): 74–9.

[13] Kinoshita Y, Takeda S, Yoshimura H, On the Dissolution of δ-ferrite into Austenite in Continuously Cast Slabs of 18-8 Stainless Steel. Tetsu-to-Hagané. 1979; 65(8): 1176–85.
[14] Raghunathan V.S, Seetharaman V, Venkadesan S, Rodriguez P, The influence of post weld heat treatments on the structure, composition and the amount of ferrite in type 316 stainless steel welds, Metall Trans A. 1979; 10(11): 1683–9.
[15] Rezayat M, Mirzadeh H, Namdar M, Parsa M.H, Unraveling the Effect of Thermomechanical Treatment on the Dissolution of Delta Ferrite in Austenitic Stainless Steels. Metall Mater Trans A. 2016; 47(2): 641–8.
[16] Kim S.H, Moon H.K, Kang T, Lee C.S, Dissolution kinetics of delta ferrite in AISI 304 stainless steel produced by strip casting process, Mater Sci Eng A. 2003; 356(1–2): 390–8.
[17] Jaafari Z, Seifoddini A, Hasani S, Rezaei-Shahreza P, Kinetic analysis of crystallization process in [(Fe0.9Ni0.1)77Mo5P9C7.5B1.5]100−xCux (x = 0.1 at.%) BMG, J Therm Anal Calorim. 2018; 134(3): 1565–74.
[18] Ansariniya M, Seifoddini A, Hasani S, (Fe0.9Ni0.1)77Mo5P9C7.5B1.5 bulk metallic glass matrix composite produced by partial crystallization: The non-isothermal kinetic analysis. J Alloys Compd. 2018; 763: 606–12.
[19] Hasani S, Jaafari Z, Seifoddini A, Rezaei-Shahreza P, Nucleation and growth of nano-crystallites in a new multicomponent Fe-based BMG during the partial crystallization process, J Therm Anal Calorim. 2021; 145(1): 109–18.
[20] Rezaei-Shahreza P, Seifoddini A, Hasani S, Thermal stability and crystallization process in a Fe-based bulk amorphous alloy: The kinetic analysis. J Non Cryst Solids. 2017; 471: 286–94.
[21] Rezaei-Shahreza P, Seifoddini A, Hasani S, Non-isothermal kinetic analysis of nano-crystallization process in (Fe41Co7Cr15Mo14Y2C15)94B6 amorphous alloy. Thermochim Acta. 2017; 652: 119–25.
[22] Hasani S, Rezaei-Shahreza P, Seifoddini A, The effect of Cu minor addition on the non-isothermal kinetic of nano-crystallites formation in Fe41Co7Cr15Mo14Y2C15B6 BMG, J Therm Anal Calorim. 2021; 143(5): 3365–75.
[23] Hasani S, Panjepour M, Shamanian M, Non-isothermal kinetic analysis of oxidation of pure aluminum powder particles, Oxid Met. 2014; 81(3–4): 299–313.
[24] Rajabi A, Mashreghi A.R, Hasani S, Non-isothermal kinetic analysis of high temperature oxidation of Ti–6Al–4V alloy, J Alloys Compd. 2020; 815.
[25] Hasani S, Shamanian M, Shafyei A, Behjati P, Szpunar J.A.A, Non-isothermal kinetic analysis on the phase transformations of Fe–Co–V alloy, Thermochim Acta, 2014; 596: 89–97.
[26] Vyazovkin S, Wight C.A, Isothermal and non-isothermal kinetics of thermally stimulated reactions of solids. Int Rev Phys Chem. 1998; 17(3): 407–33.
[27] Flynn J.H, Thermal analysis kinetics-problems, pitfalls and how to deal with them, J Therm Anal. 1988; 34(1): 367–81.
[28] Vitázek I, Šotnar M, Hrehová S, Darnadyová K, Mareček J, Isothermal Kinetic Analysis of the Thermal Decomposition of Wood Chips from an Apple Tree, Processes. 2021; 9(2): 195.